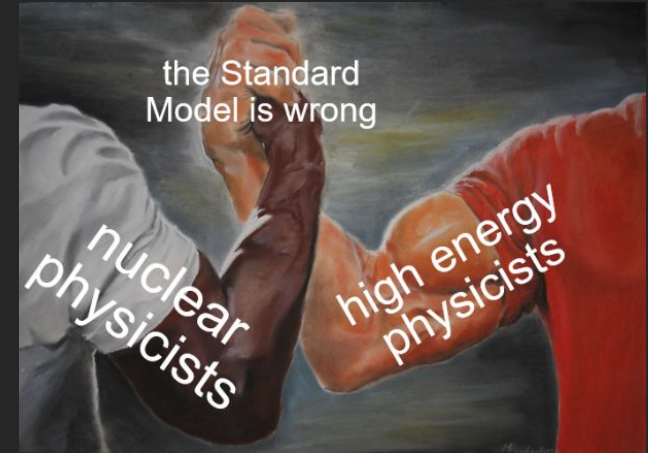




Daniel J Salvat

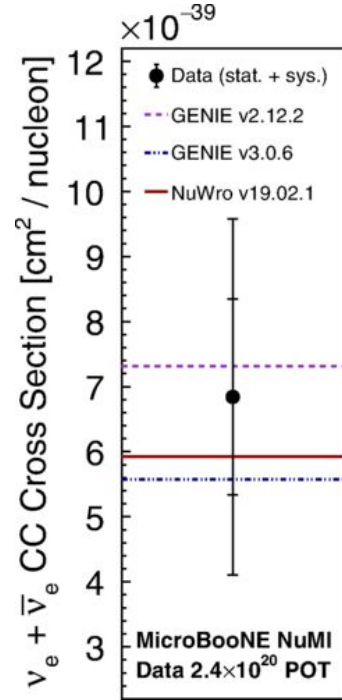
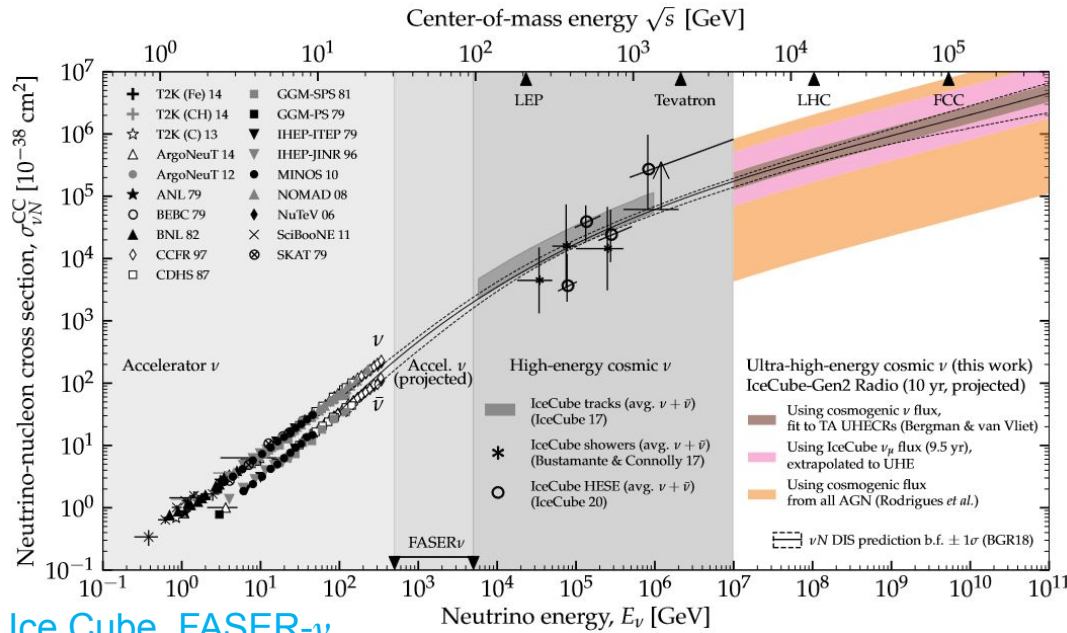
Neutrino-nuclear cross sections, beyond-standard-model physics, and accelerator-produced dark matter



Daniel J Salvat

Neutrino-nuclear cross sections, beyond-standard-model physics, and accelerator-produced dark matter

Ultra-high energy, high energy



Ice Cube, FASER- ν , ... The ultra-high-energy neutrino-nucleon cross section: measurement forecasts for an era of cosmic EeV-neutrino discovery

MicroBooNE, ICARUS, ...

Victor B. Valera* and Mauricio Bustamante†
*Niels Bohr International Academy, Niels Bohr Institute,
 University of Copenhagen, DK-2100 Copenhagen, Denmark*

Christian Glaser‡
*Department of Physics and Astronomy, Uppsala University, Uppsala, SE-752 37, Sweden
 (Dated: December 9, 2022)*

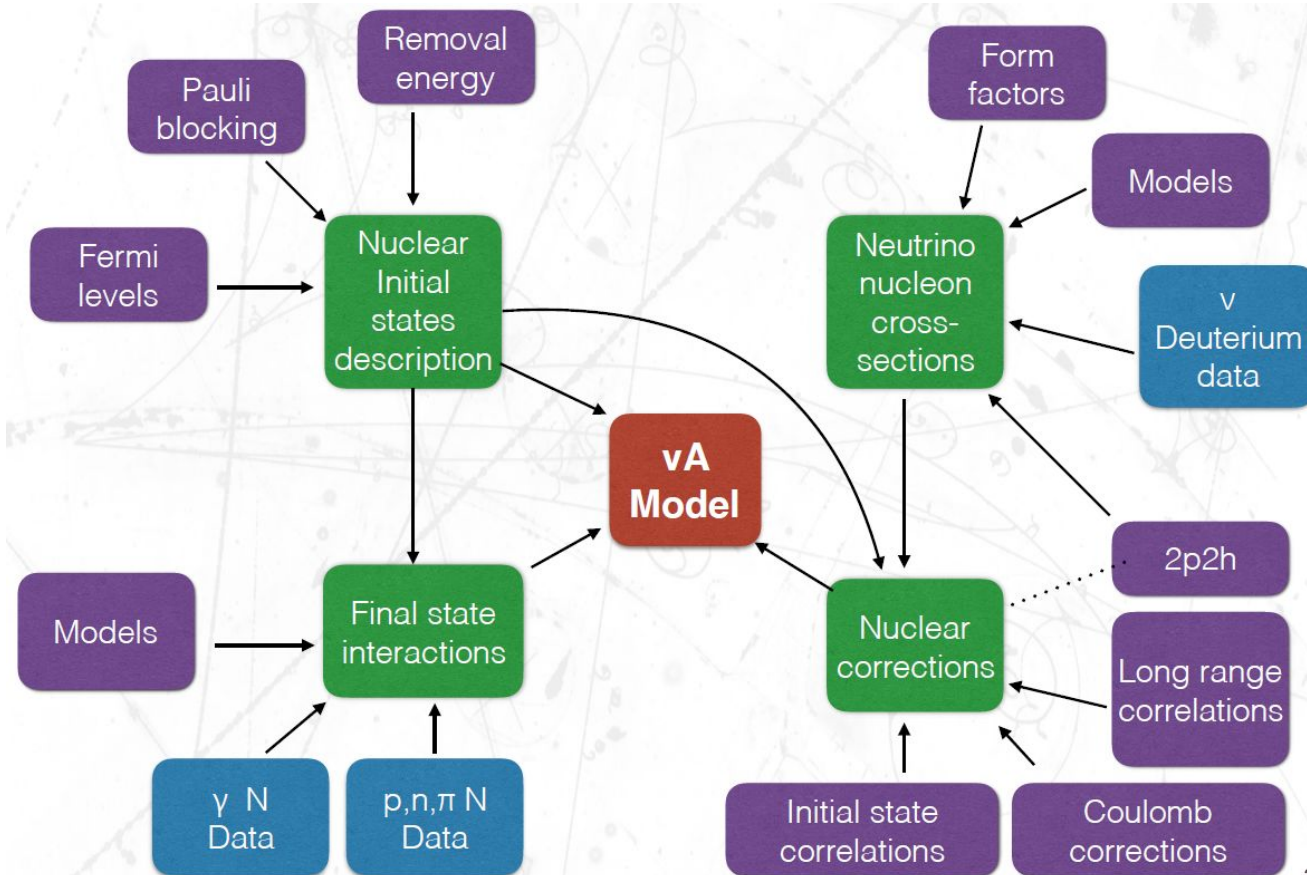
arXiv:2204.04237v3 [hep-ph]

Measurement of the flux-averaged inclusive charged-current electron neutrino and antineutrino cross section on argon using the NuMI beam and the MicroBooNE detector

P. Abratenko *et al.* (MicroBooNE Collaboration)
 Phys. Rev. D **104**, 052002 – Published 8 September 2021



Neutrino-nuclear interactions (high energy)



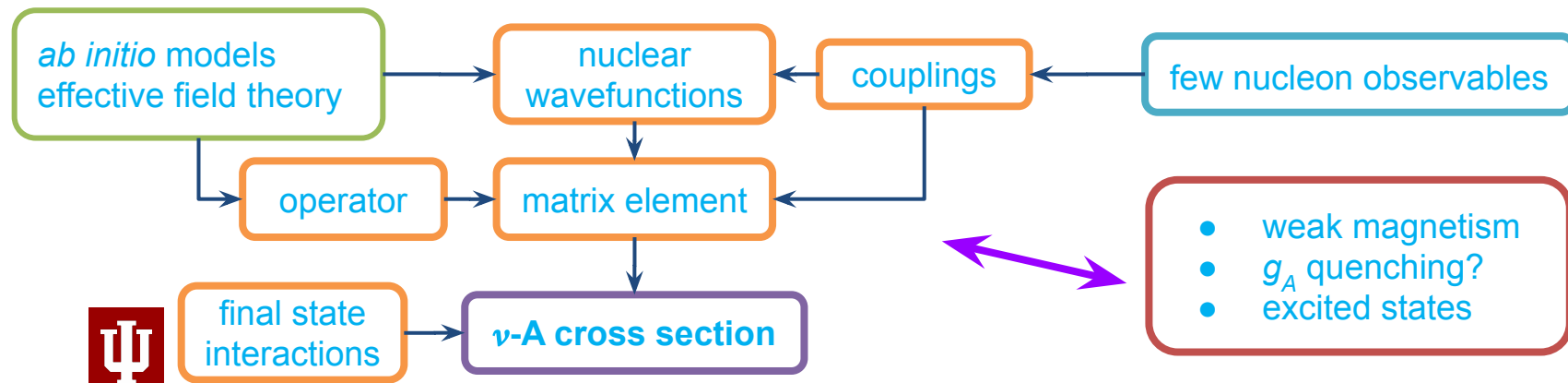
Low energy $A-\nu$ cross sections

Neutrino-nuclear interactions (low energy)

$$\langle \Psi_f | \mathcal{O} | \Psi_i \rangle$$

$$\mathcal{M} = \frac{G_F V_{ud}}{\sqrt{2}} \left[\langle \bar{n} | (\gamma_\mu f_V(0) - \gamma_\mu \gamma^5 f_A(0) - \frac{i f_P(0)}{2M_n} \sigma_{\mu\nu} q^\nu) | p \rangle \langle \bar{\nu}_e | \gamma^\mu (1 - \gamma^5) | e \rangle \right]$$

- $0\nu\beta\beta$
- μ -capture



Neutrino-nuclear interactions (low energy)

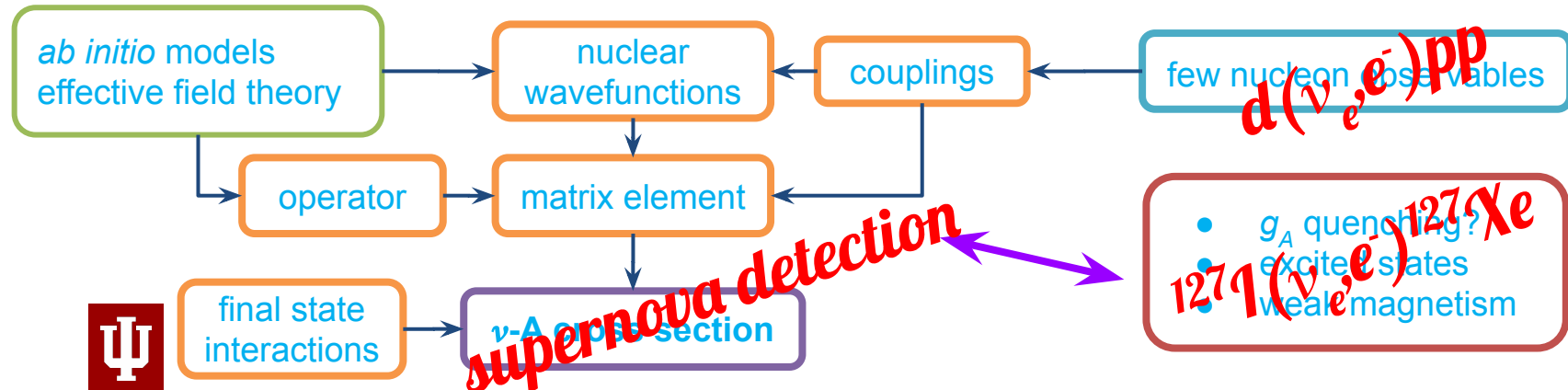
$$\langle \Psi_f | \mathcal{O} | \Psi_i \rangle$$

$$\mathcal{M} = \frac{G_F V_{ud}}{\sqrt{2}} \left[\langle \bar{n} | (\gamma_\mu f_V(0) - \gamma_\mu \gamma^5 f_A(0) - \frac{i f_P(0)}{2M_n} \sigma_{\mu\nu} q^\nu) | p \rangle \langle i | \right]$$

Muon-capture strength functions in intermediate nuclei of $0\nu\beta\beta$ decays

L. Jokiniemi and J. Suhonen
Phys. Rev. C **100**, 014619 – Published 31 July 2019

- $0\nu\beta\beta$
- μ -capture



Existing data

Isotope	Reaction Channel	Source	Experiment	Measurement (10^{-42} cm ²)	Theory (10^{-42} cm ²)
² H	² H(ν_e, e^-)pp	Stopped π/μ	LAMPF	$52 \pm 18(\text{tot})$	54 (IA) (Tatara <i>et al.</i> , 1990)
¹² C	¹² C(ν_e, e^-) ¹² N _{g.s.}	Stopped π/μ	KARMEN	$9.1 \pm 0.5(\text{stat}) \pm 0.8(\text{sys})$	9.4 [Multipole](Donnelly and Peccei, 1979)
		Stopped π/μ	E225	$10.5 \pm 1.0(\text{stat}) \pm 1.0(\text{sys})$	9.2 [EPT] (Fukugita <i>et al.</i> , 1988).
		Stopped π/μ	LSND	$8.9 \pm 0.3(\text{stat}) \pm 0.9(\text{sys})$	8.9 [CRPA] (Kolbe <i>et al.</i> , 1999b)
	¹² C(ν_e, e^-) ¹² N*	Stopped π/μ	KARMEN	$5.1 \pm 0.6(\text{stat}) \pm 0.5(\text{sys})$	5.4-5.6 [CRPA] (Kolbe <i>et al.</i> , 1999b)
		Stopped π/μ	E225	$3.6 \pm 2.0(\text{tot})$	4.1 [Shell] (Hayes and S, 2000)
		Stopped π/μ	LSND	$4.3 \pm 0.4(\text{stat}) \pm 0.6(\text{sys})$	
¹² C(ν_μ, ν_μ) ¹² C*	Stopped π/μ	KARMEN	$3.2 \pm 0.5(\text{stat}) \pm 0.4(\text{sys})$	2.8 [CRPA] (Kolbe <i>et al.</i> , 1999b)	
¹² C(ν, ν) ¹² C*	Stopped π/μ	KARMEN	$10.5 \pm 1.0(\text{stat}) \pm 0.9(\text{sys})$	10.5 [CRPA] (Kolbe <i>et al.</i> , 1999b)	
¹² C(ν_μ, μ^-)X	Decay in Flight	LSND		$1060 \pm 30(\text{stat}) \pm 180(\text{sys})$	1750-1780 [CRPA] (Kolbe <i>et al.</i> , 1999b) 1380 [Shell] (Hayes and S, 2000) 1115 [Green's Function] (Meucci <i>et al.</i> , 2004)
				$56 \pm 8(\text{stat}) \pm 10(\text{sys})$	68-73 [CRPA] (Kolbe <i>et al.</i> , 1999b) 56 [Shell] (Hayes and S, 2000)
⁵⁶ Fe	⁵⁶ Fe(ν_e, e^-) ⁵⁶ Co	Stopped π/μ	KARMEN	$256 \pm 108(\text{stat}) \pm 43(\text{sys})$	264 [Shell] (Kolbe <i>et al.</i> , 1999a)
⁷¹ Ga	⁷¹ Ga(ν_e, e^-) ⁷¹ Ge	⁵¹ Cr source	GALLEX, ave.	$0.0054 \pm 0.0009(\text{tot})$	0.0058 [Shell] (Haxton, 1998)
		⁵¹ Cr	SAGE	$0.0055 \pm 0.0007(\text{tot})$	
		³⁷ Ar source	SAGE	$0.0055 \pm 0.0006(\text{tot})$	0.0070 [Shell] (Bahcall, 1997)
¹²⁷ I	¹²⁷ I(ν_e, e^-) ¹²⁷ Xe	Stopped π/μ	LSND	$284 \pm 91(\text{stat}) \pm 25(\text{sys})$	210-310 [Quasi-particle] (Engel <i>et al.</i> , 1994)

All's loud on the theory front

Coherent elastic neutrino-nucleus scattering on ^{40}Ar from first principles

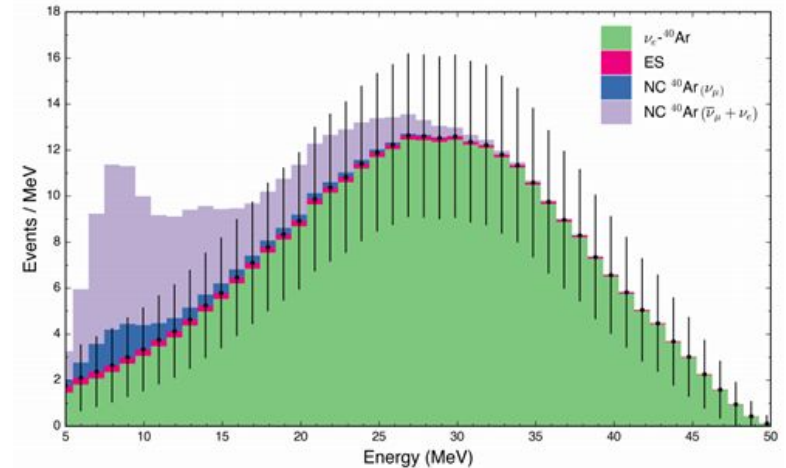
C. G. Payne,¹ S. Bacca,¹ G. Hagen,^{2,3,*} W. Jiang,^{3,2} and T. Papenbrock^{3,2}

¹*Institut für Kernphysik and PRISMA⁺ Cluster of Excellence,
Johannes Gutenberg-Universität, 55128 Mainz, Germany*

²*Physics Division, Oak Ridge National Laboratory, Oak Ridge, TN 37831, USA*

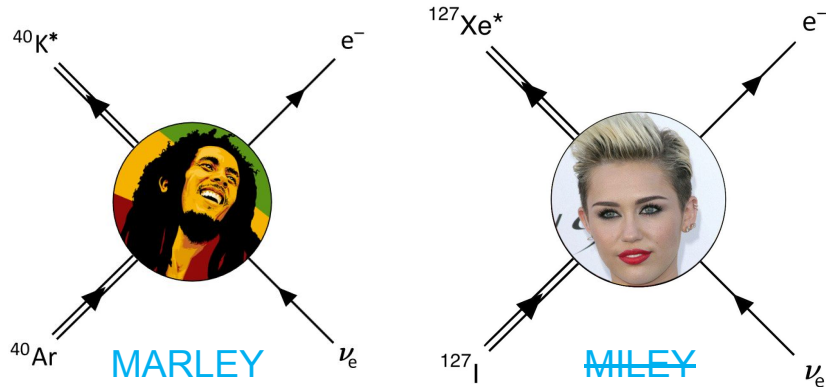
³*Department of Physics and Astronomy, University of Tennessee, Knoxville, TN 37996, USA*

Coherent elastic neutrino scattering on the ^{40}Ar nucleus is computed with coupled-cluster theory based on nuclear Hamiltonians inspired by effective field theories of quantum chromodynamics. Our approach is validated by calculating the charge form factor and comparing it to data from electron scattering. We make predictions for the weak form factor, the neutron radius, and the neutron skin, and estimate systematic uncertainties. The neutron-skin thickness of ^{40}Ar is consistent with results from density functional theory. Precision measurements from coherent elastic neutrino-nucleus scattering could potentially be used to extract these observables and help to constrain nuclear models.



Low energy event generators

- Higher energy neutrino efforts (Genie, NEUT, NuWro, GiBUU, ...)
- Low energy generators often motivated by SN, nucleus-specific (sntools, SKSNSim, newton, *JUNO generator?* ...)
- Model of Argon Reaction Low Energy Yields (MARLEY) adding more nuclei, benchmarking with new data...



Supernova neutrinos

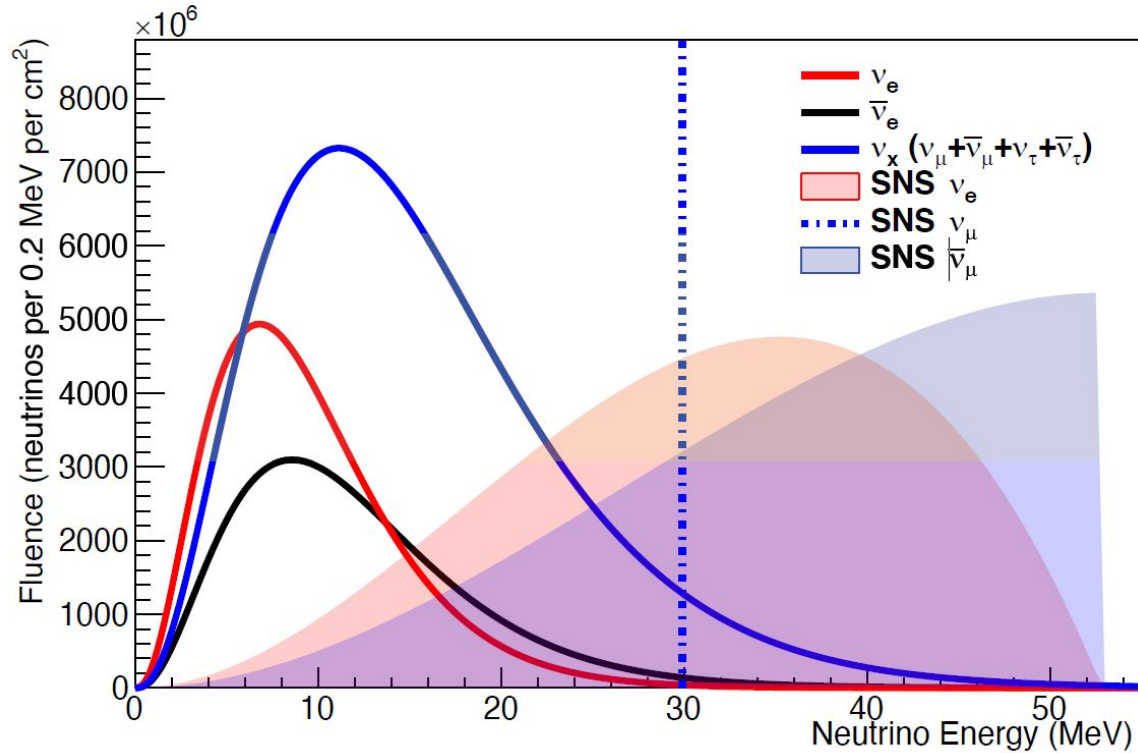
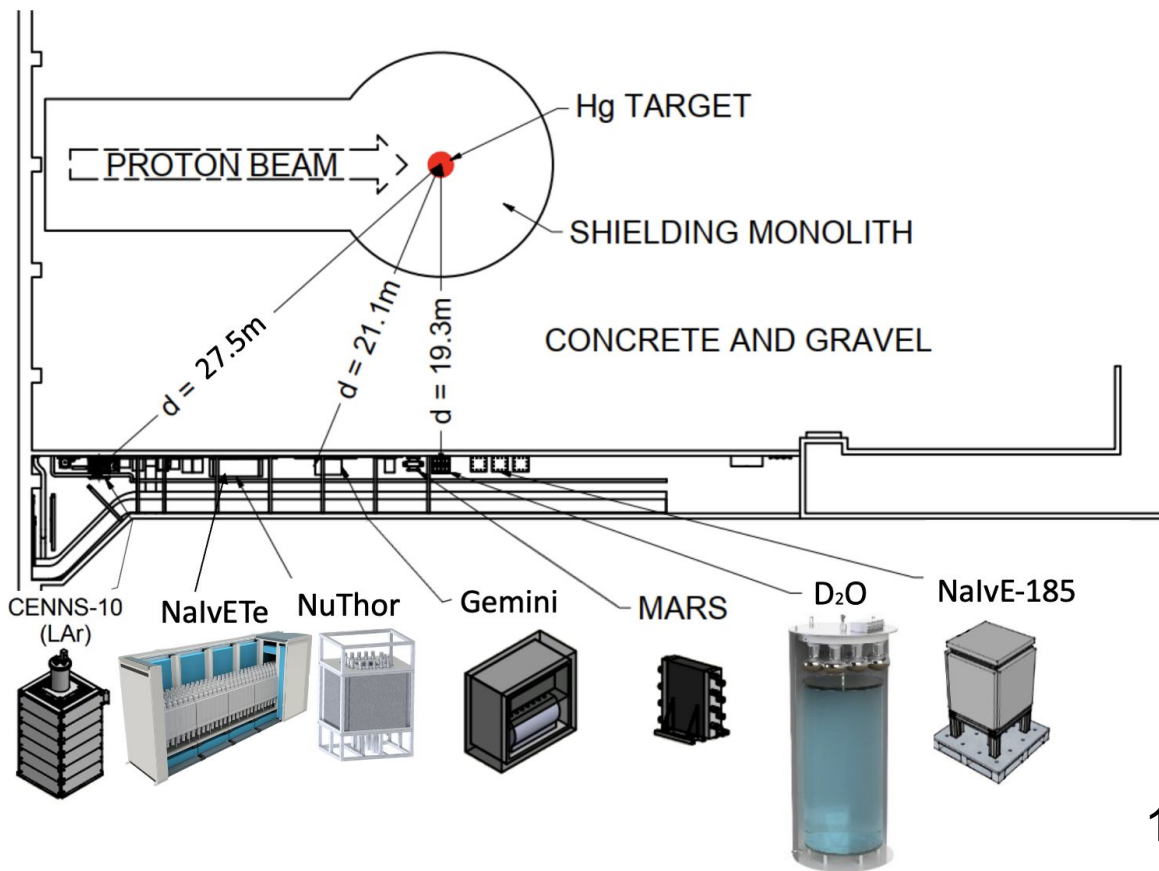
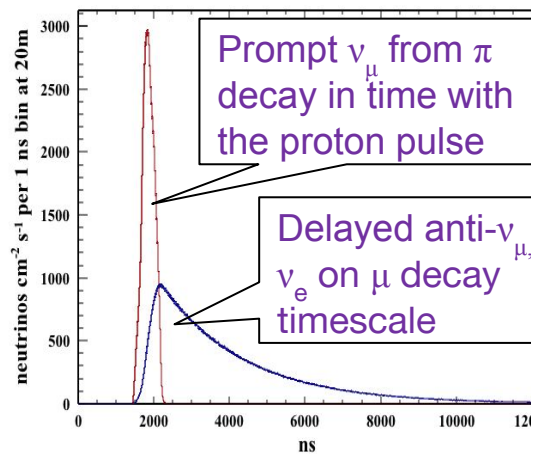
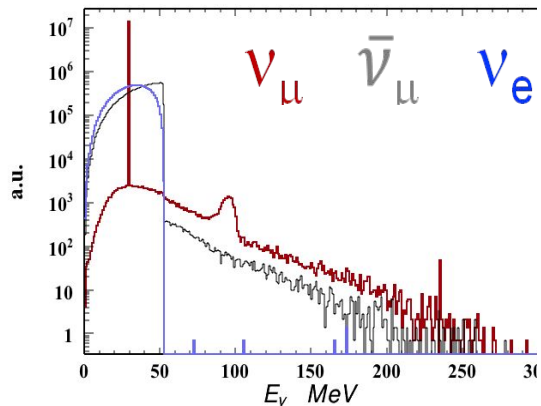
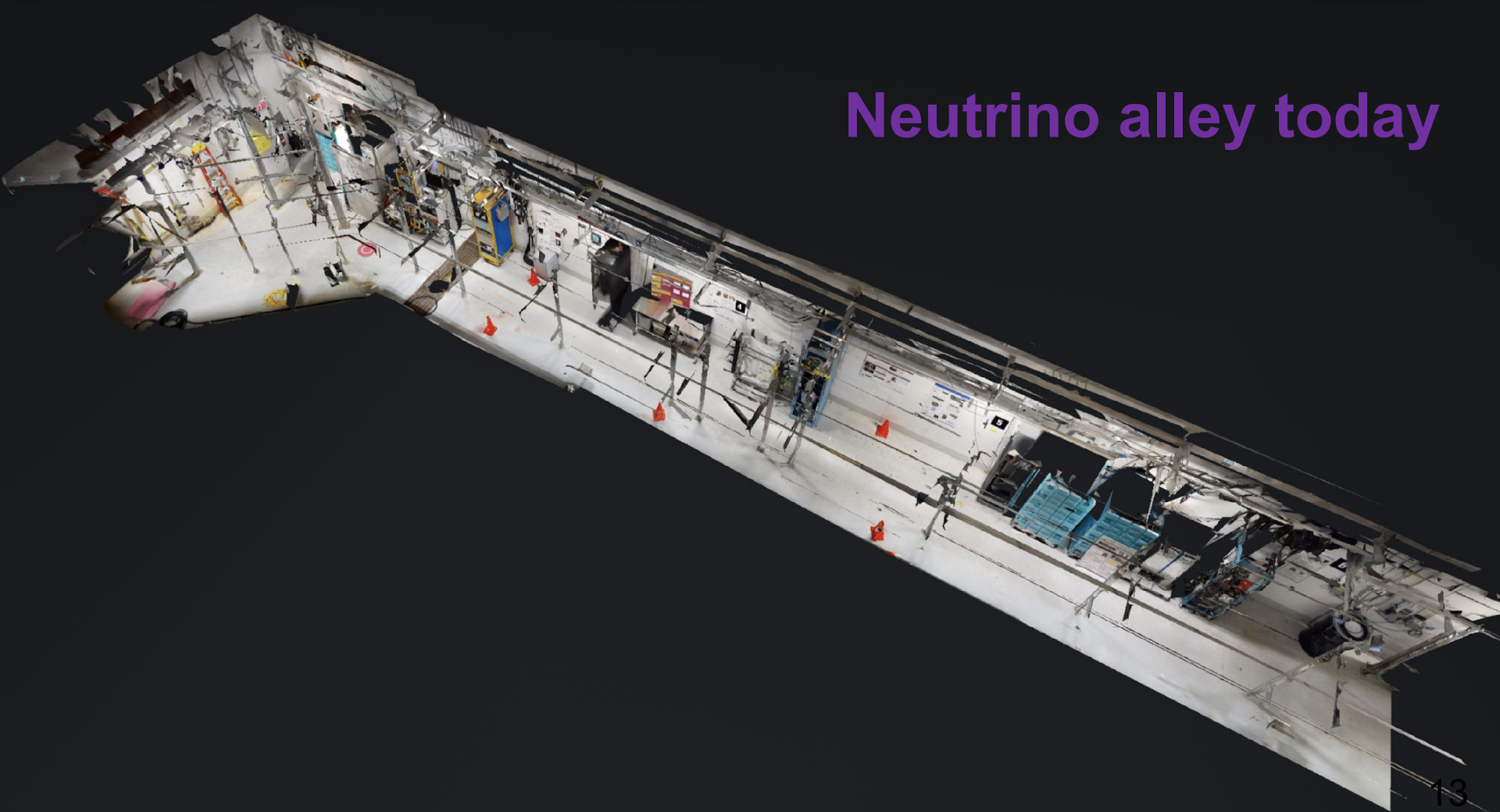


[image by K. Scholberg]

COHERENT @ ORNL SNS

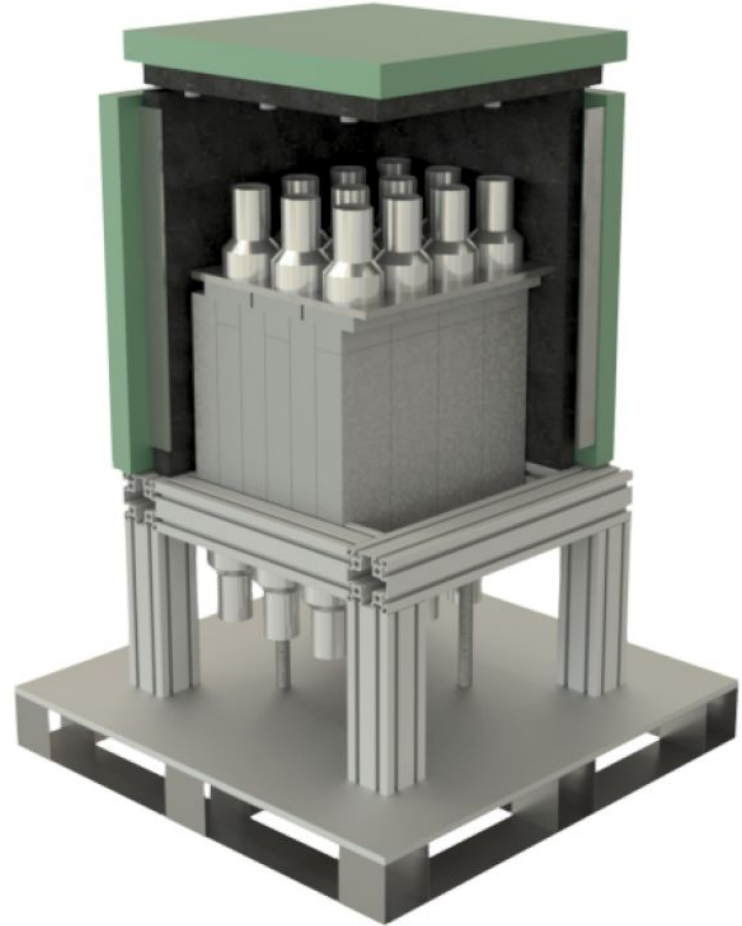


Neutrino alley today

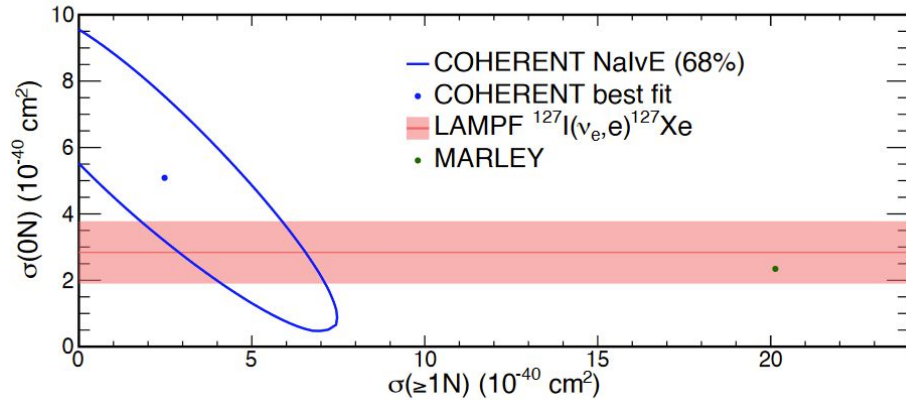


NalvE-185

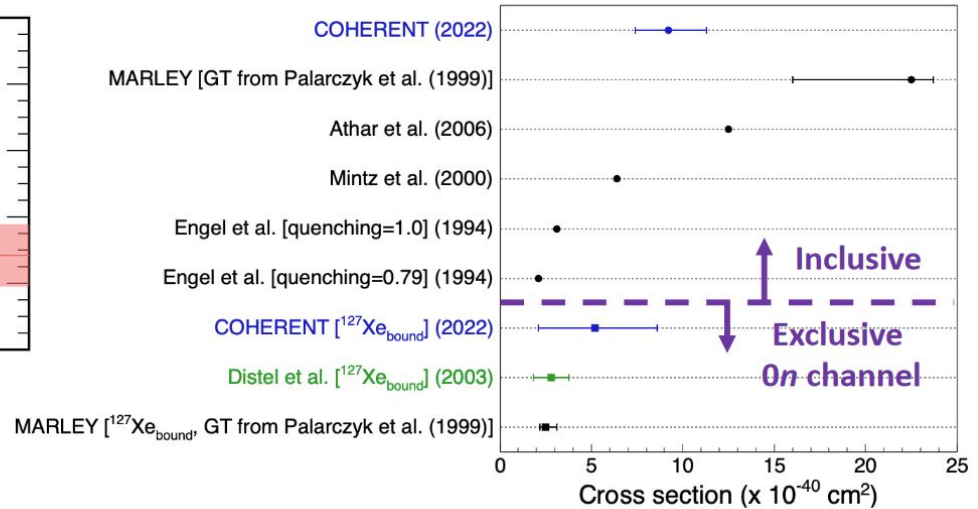
- 7.7kg NaI[Tl] detectors
- 185 kg total mass
- CC interactions on Na, I



NalvE-185



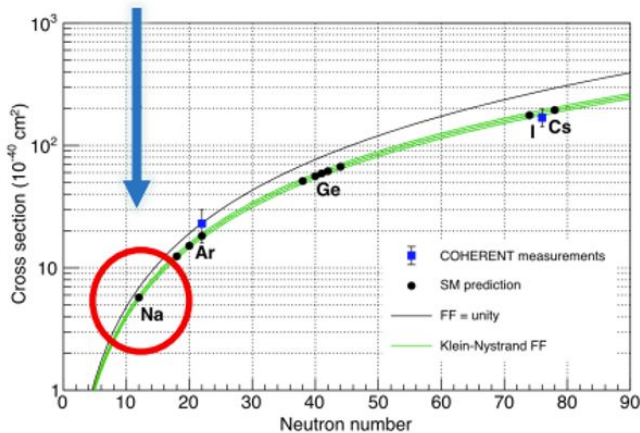
^{127}I Flux-Averaged DAR Cross Sections



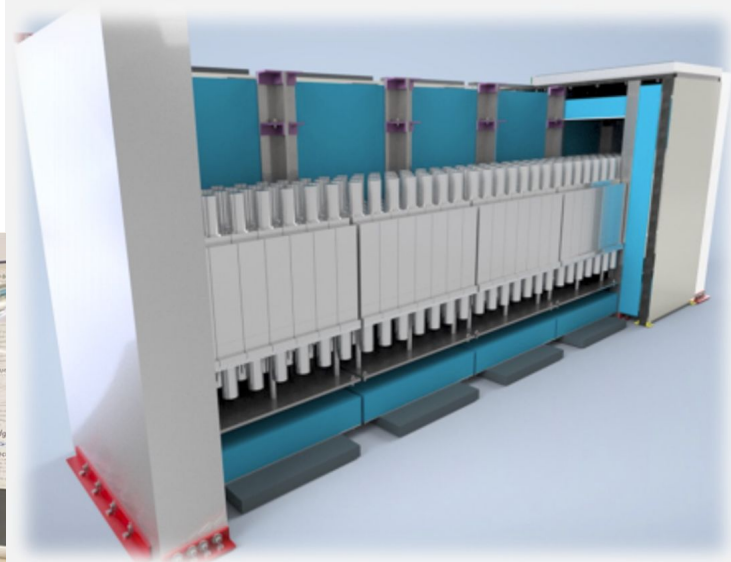
NalvETe



- 7.7kg NaI[Tl] detectors
- 63 crystals per module
- 2.4 tons being deployed
- CEvNS on Na
- CC interactions on Na, I

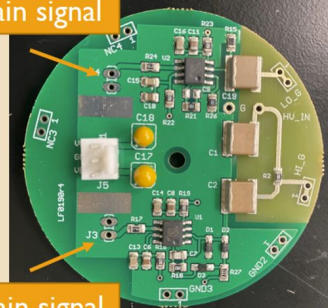


One module test assembly at Duke



Dual-gain base design \rightarrow low-energy CEvNS and high-energy CC signals can be read out from *same* crystal

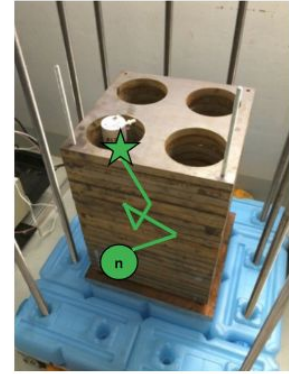
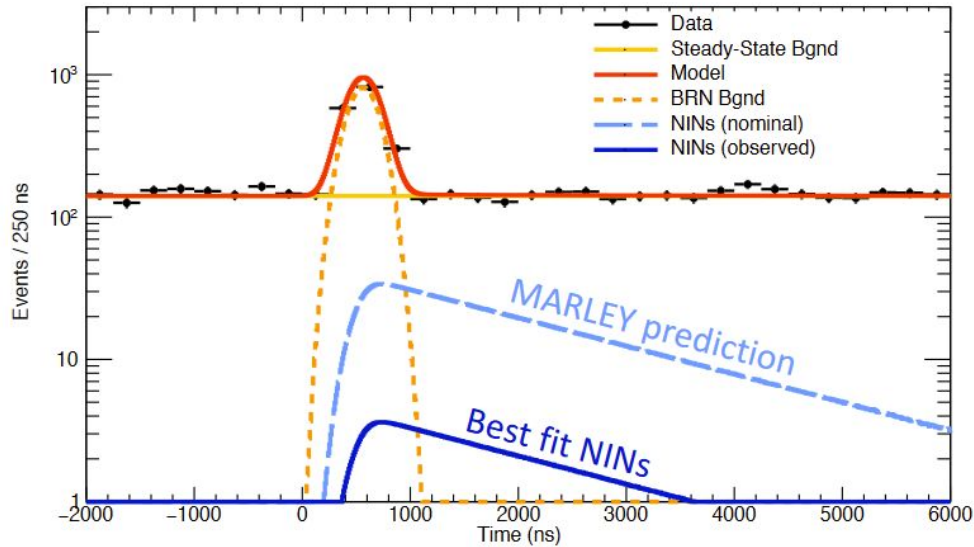
Low-gain signal



High-gain signal



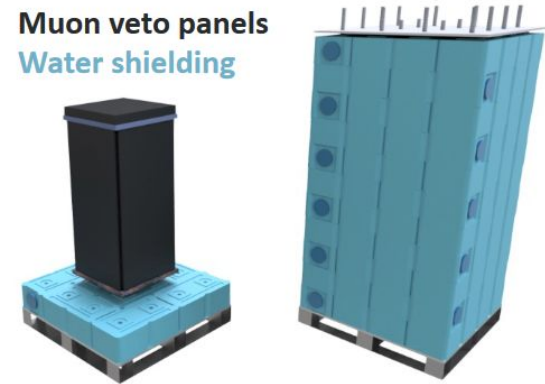
Neutrino induced neutrons



LS detectors
Pb target



Muon veto panels
Water shielding



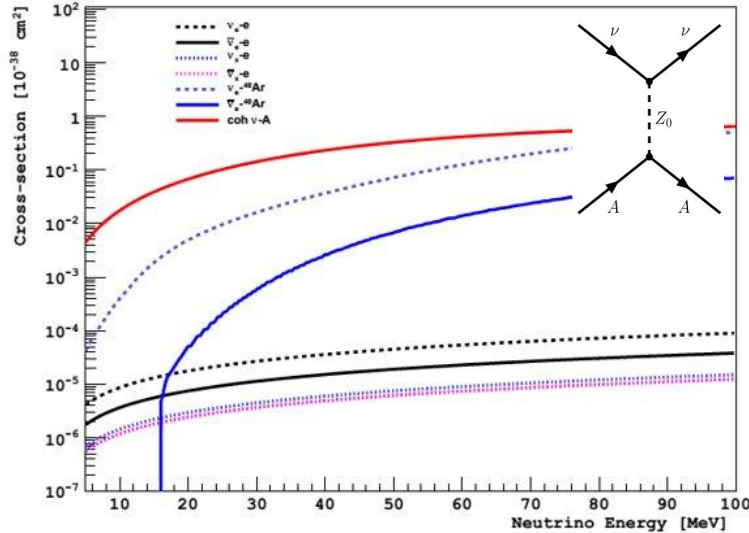


CEvNS

Coherent Elastic Neutrino-Nucleus Scattering

$$\lambda = \frac{\hbar}{p} = \frac{1200 \text{ MeV fm}}{50 \text{ MeV}} \sim 25 \text{ fm}$$

$$\frac{d\sigma}{dT_{coh}} = \frac{G_f^2 M}{2\pi} G_V^2 \left[1 + \left(1 - \frac{T}{E_\nu} \right)^2 - \frac{MT}{E_\nu^2} \right]$$



$$G_V = (g_V^p Z + g_V^n N) F_{\text{nucl}}^V(Q^2)$$

small proton $\sigma \sim N^2$ \sim few-%
 weak charge uncertainty

CEvNS cross section ingredients

$$\frac{d\sigma}{dT_{coh}} = \frac{G_f^2 M}{2\pi} G_V^2 \left[1 + \left(1 - \frac{T}{E_\nu} \right)^2 - \frac{MT}{E_\nu^2} \right]$$

Neutrino-nucleus coherent scattering as a probe of neutron density distributions

Kelly Patton, Jonathan Engel, Gail C. McLaughlin, and Nicolas Schunck
Phys. Rev. C **86**, 024612 – Published 30 August 2012

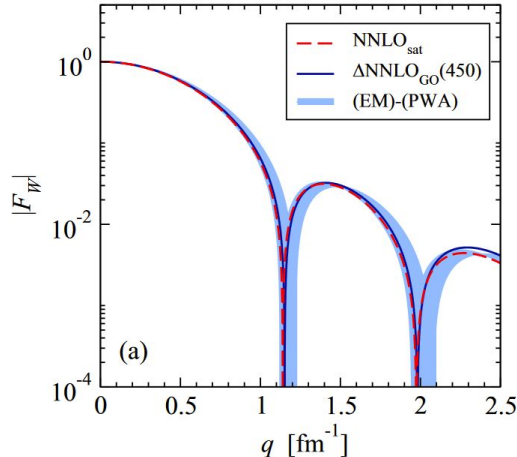
$$G_V = (g_V^p Z + g_V^n N) F_{\text{nucl}}^V(Q^2)$$

Nuclear Structure Physics in Coherent Elastic Neutrino-Nucleus Scattering

N. Van Dessel,¹ V. Pandey,^{2,*} H. Ray,² and N. Jachowicz^{1,†}

¹Department of Physics and Astronomy, Ghent University, Proeftuinstraat 86, B-9000 Gent, Belgium

²Department of Physics, University of Florida, Gainesville, FL 32611, USA



C. G. PAYNE *et al.*

PHYSICAL REVIEW C **100**, 061304(R) (2019)

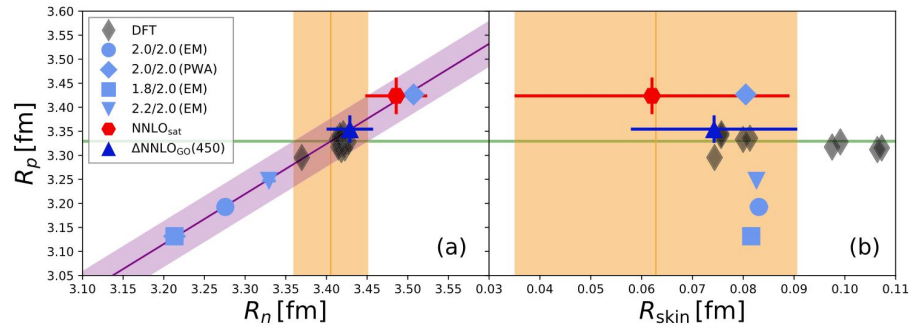


FIG. 3. Correlation (a) between R_p and R_n and (b) between R_p and R_{skin} for various Hamiltonians. The experimental R_p is also shown by the horizontal green line [48] as well as the DFT data [49] by the diamonds.

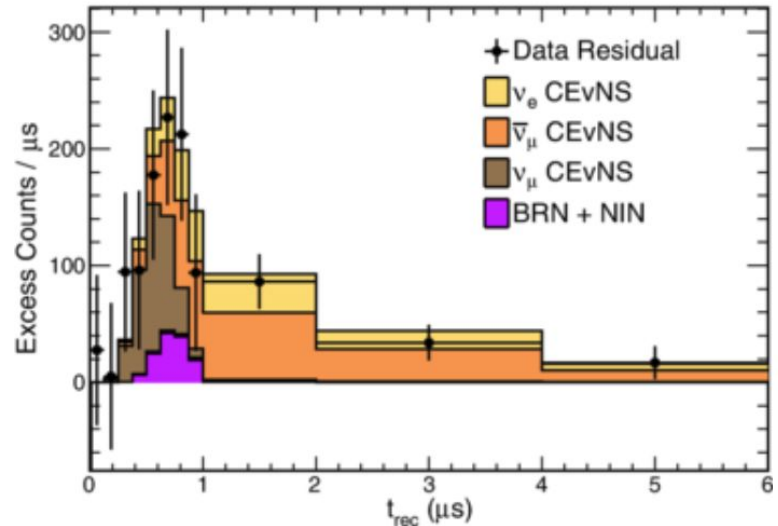
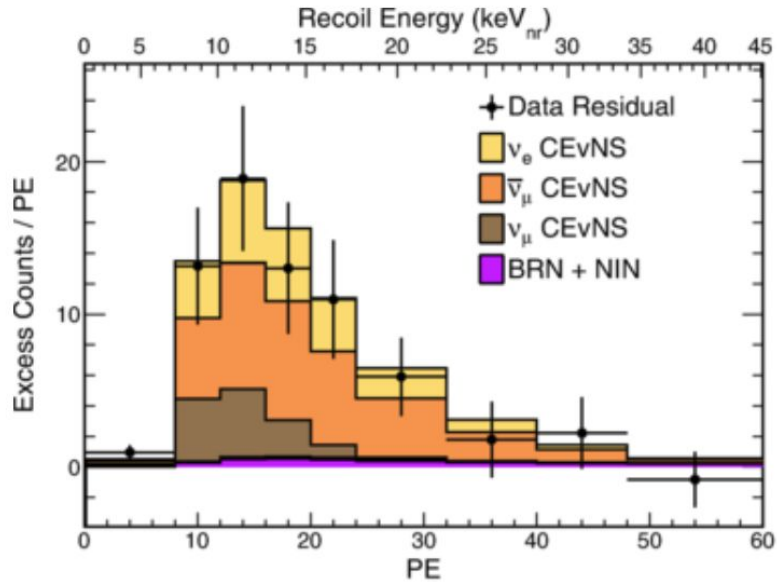
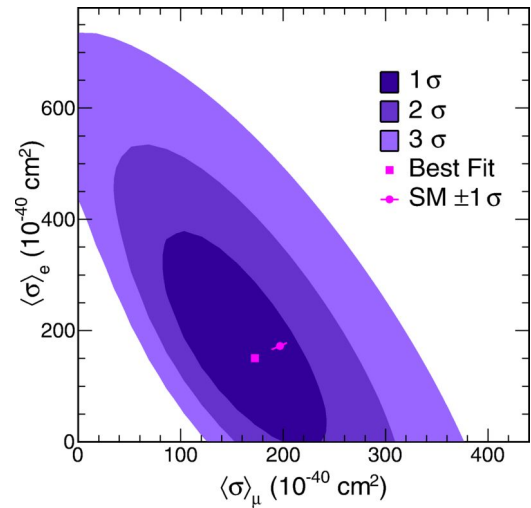
CEvNS around the globe

Experiments

- Stopped-pion beams
- Nuclear reactors



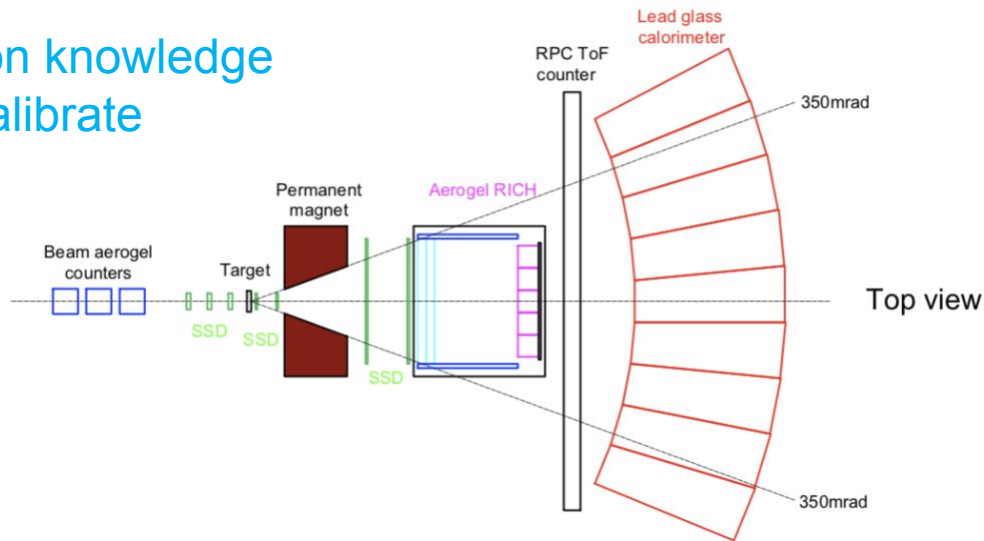
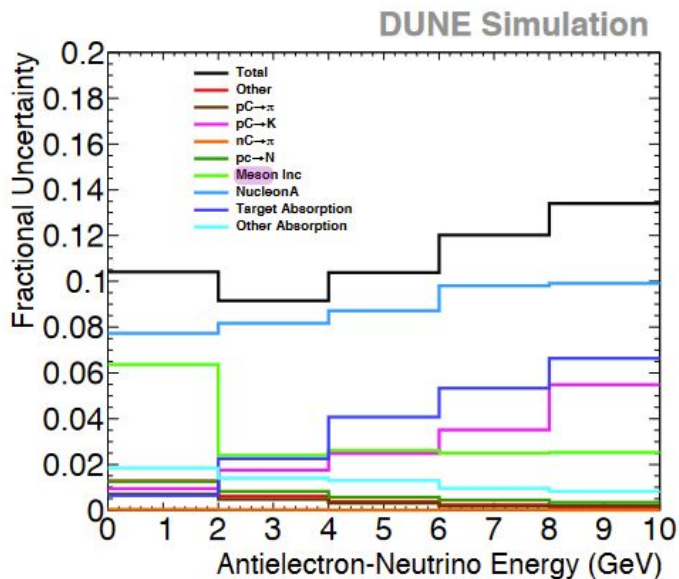
Separating neutrino flavors



Neutrino flux

Flux improvements

- reactor neutrino anomaly
- improve modeling, hadron production knowledge
- use theoretically clean channel to calibrate



Measurement of proton-carbon forward scattering in a proof-of-principle test of the EMPHATIC spectrometer

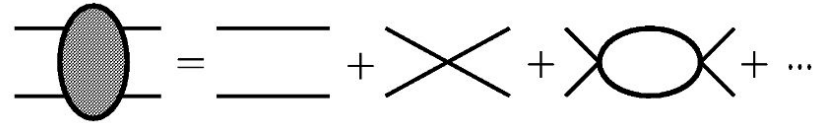
M. Pavin *et al.* (EMPHATIC Collaboration)

Phys. Rev. D **106**, 112008 – Published 23 December 2022

ν -d scattering for flux calibration

$d(\nu_e, e^-)pp$

- Use *precisely predicted cross section* to determine neutrino flux
- Systematic treatment of neutrino-deuteron cross-section
- Leveraged for Sudbury Neutrino Observatory
- Modern pionless-EFT and chiral-PT calculations



$$\sigma(\nu(\bar{\nu})d \rightarrow \nu(\bar{\nu})np) = 0.999 \pm 0.026 + 0.013L_{1,A} + 10^{-5} \Delta s (\pm 0.5 \pm 1.2\mu_s + 6.3\Delta s - 4.6L_{2,A})$$

Weak interaction processes on deuterium: Muon capture and neutrino reactions

Naoko Tataru, Y. Kohyama, and K. Kubodera
Phys. Rev. C **42**, 1694 – Published 1 October 1990

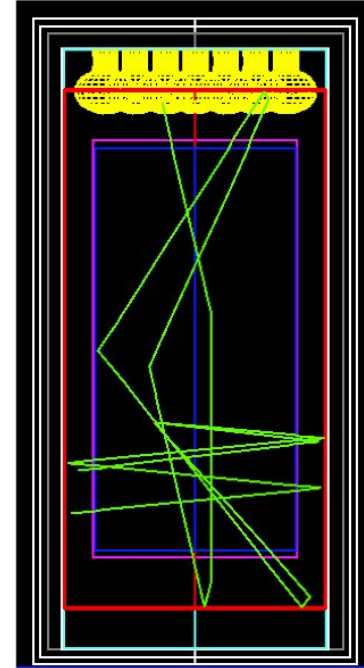
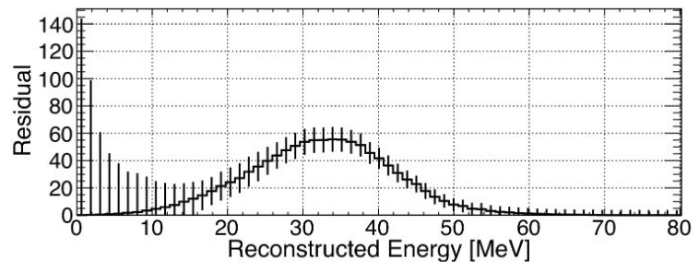
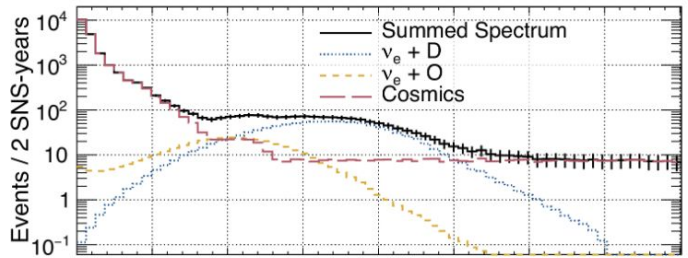
Elastic and inelastic neutrino–deuteron scattering in effective field theory

Malcolm Butler^{a,1}, Jiunn-Wei Chen^{b,2}



COHERENT D₂O detector

- two 670-kg modules
- Can achieve ~few-% sensitivity after 3 years
- D₂O available
- First module deployed, first light with H₂O



Journal of Instrumentation

PAPER

A D₂O detector for flux normalization of a pion decay-at-rest neutrino source

COHERENT collaboration, D. Akimov¹, P. An^{2,3}, C. Awe^{2,3}, P.S. Barbeau^{2,3}, B. Becker⁴, V. Belov^{5,1}, I. Bernardi⁴, M.A. Blackston⁶, A. Bolozdynya¹ [Show full author list](#)

Published 16 August 2021 • © 2021 IOP Publishing Ltd and Sissa Medialab

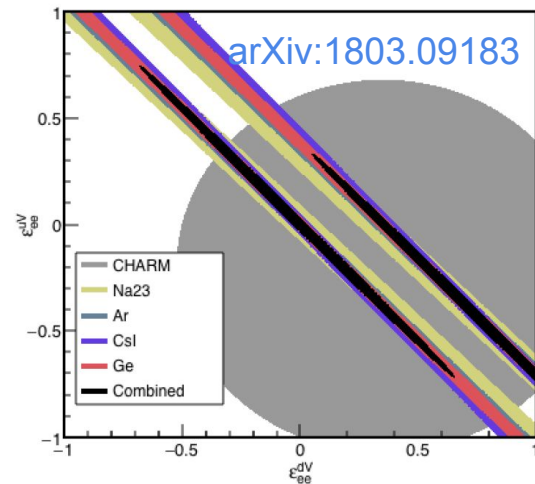
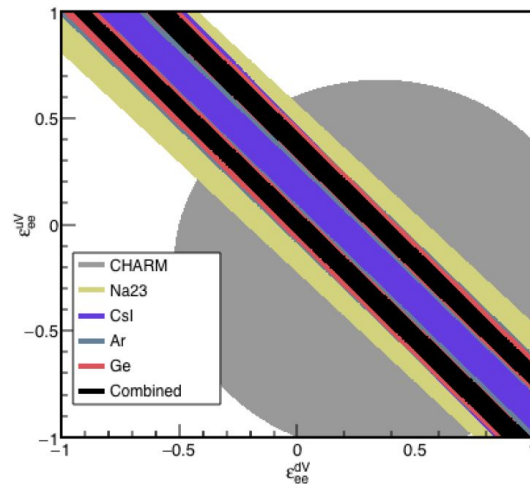
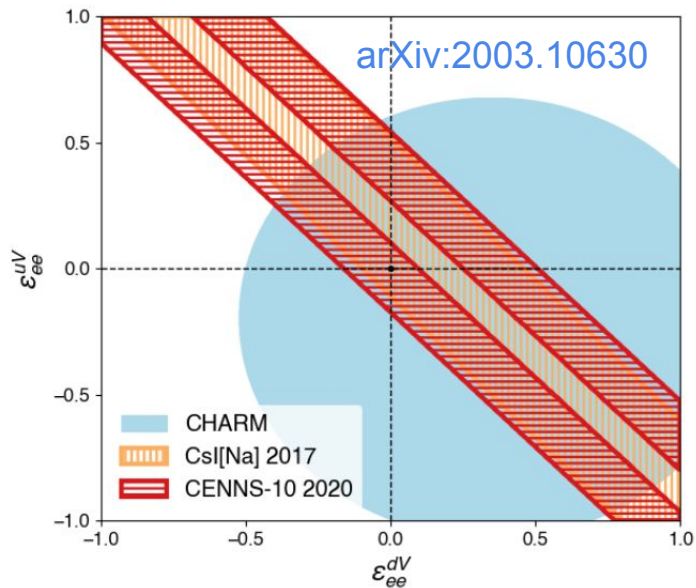
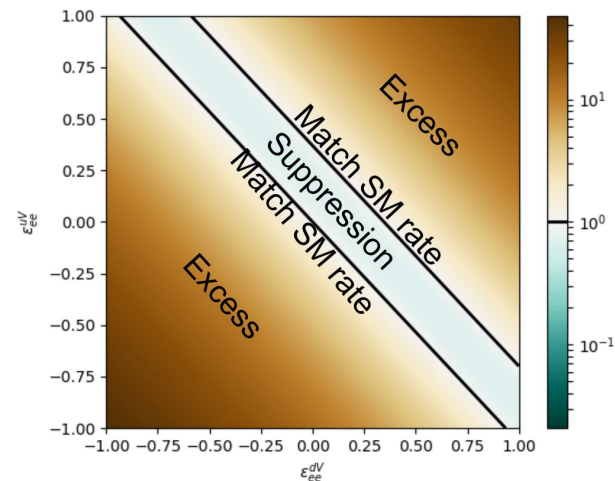


New physics

Non-standard interactions

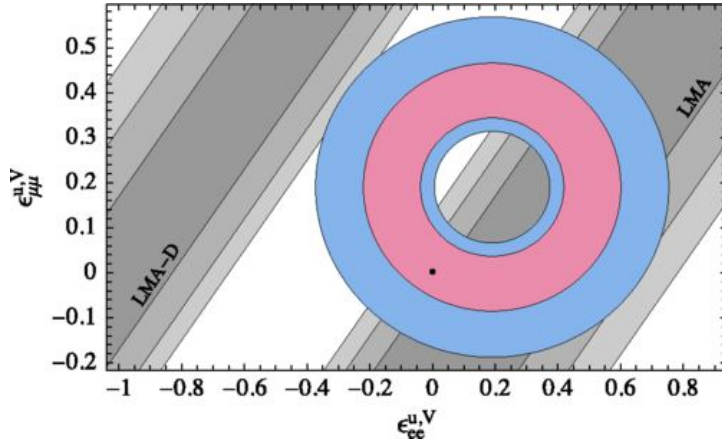
$$\mathcal{L}_{\text{NSI}} = -2\sqrt{2}G_F \sum_{f,P,\alpha,\beta} \epsilon_{\alpha\beta}^{f,P} (\bar{\nu}_\alpha \gamma^\mu P_L \nu_\beta) (\bar{f} \gamma_\mu P f)$$

$$Q_W^2 \rightarrow Q_{\text{NSI}}^2 = 4 \left[N \left(-\frac{1}{2} + \epsilon_{ee}^{uV} + 2\epsilon_{ee}^{dV} \right) + Z \left(\frac{1}{2} - 2\sin^2 \theta_W + 2\epsilon_{ee}^{uV} + \epsilon_{ee}^{dV} \right) \right]^2 + 4 \left[N (\epsilon_{e\tau}^{uV} + 2\epsilon_{e\tau}^{dV}) + Z (2\epsilon_{e\tau}^{uV} + \epsilon_{e\tau}^{dV}) \right]^2.$$

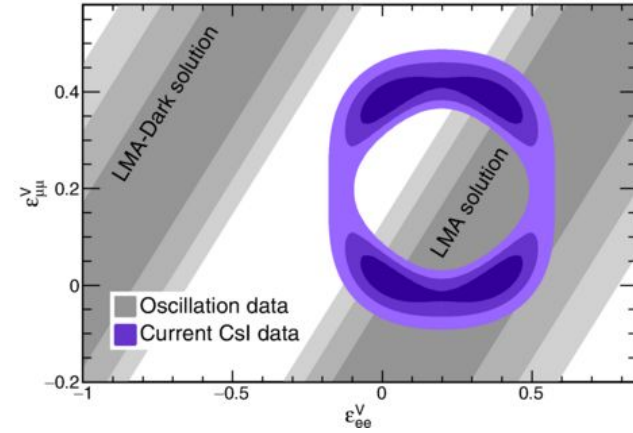


See also: O.G. Miranda, *et al.* arXiv:2003.12050v3 (2020)

LMA-Dark solution



*CEvNS compliments oscillation data
to break LMA-D degeneracy*



Constraints from CsI result

PHYSICAL REVIEW D **96**, 115007 (2017)

COHERENT enlightenment of the neutrino dark side

Pilar Coloma,^{1,*} M. C. Gonzalez-Garcia,^{2,3,4,†} Michele Maltoni,^{5,‡} and Thomas Schwetz^{6,§}



Scalar and tensor currents

$$\frac{d\sigma_a^\beta}{dE_r} = \frac{G_F^2}{4\pi} M_a N_a^2 [(\xi_S^\beta)^2 \frac{E_r}{E_{r,\max}} + (\xi_V^\beta)^2 (1 - \frac{E_r}{E_{r,\max}} - \frac{E_r}{E_\nu}) + (\xi_T^\beta)^2 (1 - \frac{E_r}{2E_{r,\max}} - \frac{E_r}{E_\nu})] F^2(q^2)$$

Scalar and tensor neutrino interactions

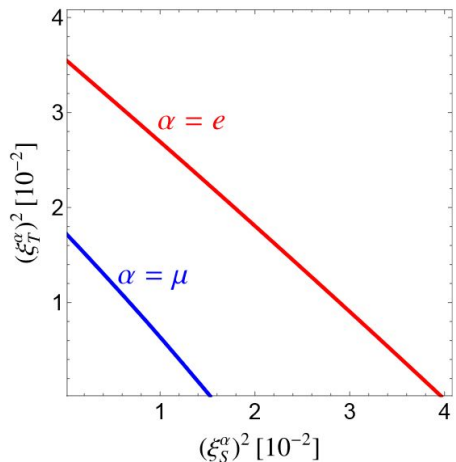


Figure 4: Projected 90% C.L. upper bounds from the future COHERENT experiment with a 610 kg fiducial mass of LAr.

arXiv:2004.13869 [hep-ph] (2020)

Tao Han,^a Jiajun Liao,^b Hongkai Liu,^a Danny Marfatia^c

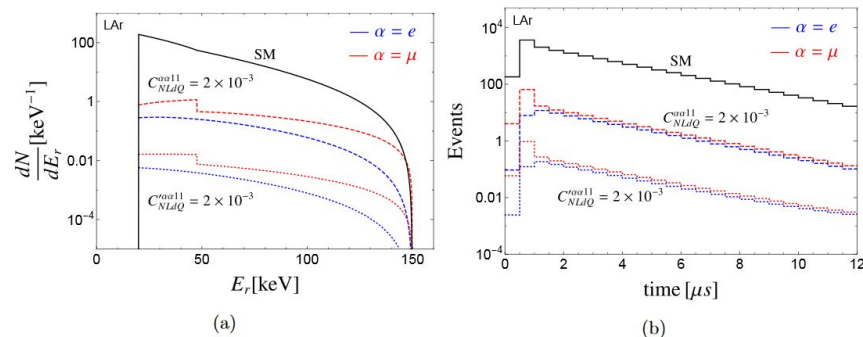


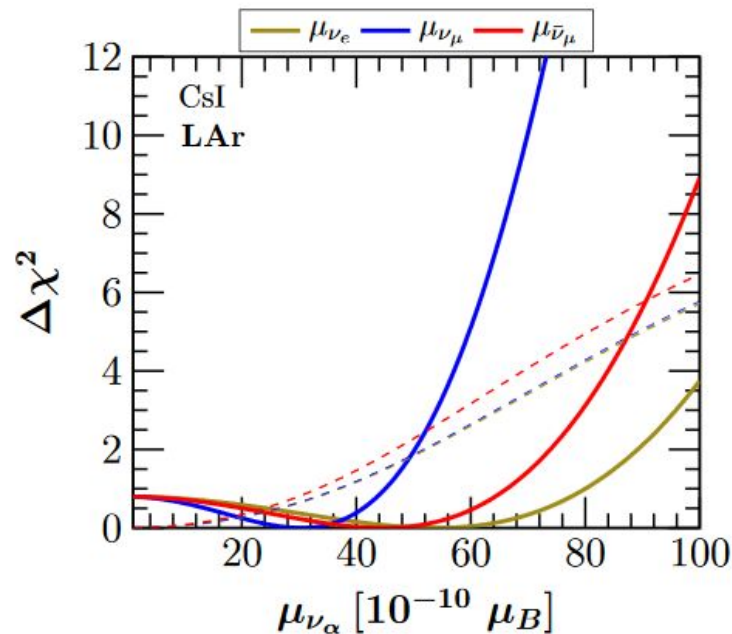
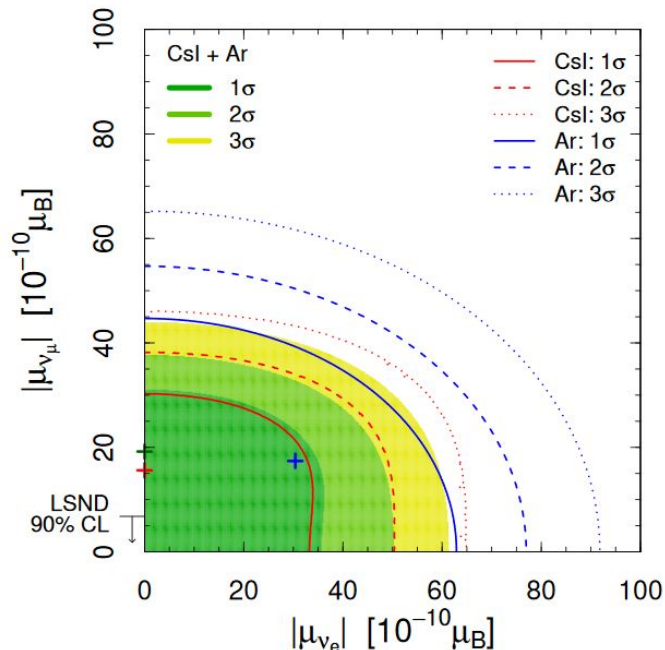
Figure 3: The recoil energy (left) and temporal (right) distributions in a future COHERENT LAr detector. Threshold effects are included. The black solid lines are the SM case including all flavors. The blue (red) curves correspond to the electron (muon+antimuon) flavor contributions. The dashed (dotted) curves correspond to the contributions from the scalar (tensor) interactions with C_{NLdQ} (C'_{NLdQ}) = 2×10^{-3} .

O. G. Miranda,^{1,*} D. K. Papoulias,^{2,†} G. Sanchez Garcia,^{1,‡}
O. Sanders,^{1,§} M. Tórtola,^{3,¶} and J. W. F. Valle^{3,**}

ν magnetic moment

Physics results from the first COHERENT observation of CEvNS in argon and their combination with cesium-iodide data

M. Cadeddu,^{1,¶} F. Dordei,^{1,¶} C. Giunti,^{2,¶} Y.F. Li,^{3,4,§} E. Picciau,^{5,6,¶} and Y.Y. Zhang^{3,4,¶}



$$\frac{d\sigma_{\nu MM}^{ij}}{dt} = \frac{e^2}{8\pi\lambda} \left| \frac{\mu_{ij}}{\mu_B} \right|^2 Z^2 F_Z^2(q^2) \left[\frac{1}{t} (2\lambda + 4M^2 m_i^2 + 2A\Delta + 2M^2\Delta + \Delta^2) + (2A + \Delta) + \frac{2M^2\Delta^2}{t^2} \right]$$

Neutrino charge, charge radii

Physics results from the first COHERENT observation of CE ν NS in argon and their combination with cesium-iodide data

M. Cadeddu,^{1,*} F. Dordei,^{1,†} C. Giunti,^{2,‡} Y.F. Li,^{3,4,§} E. Picciau,^{5,6,¶} and Y.Y. Zhang^{3,4,**}

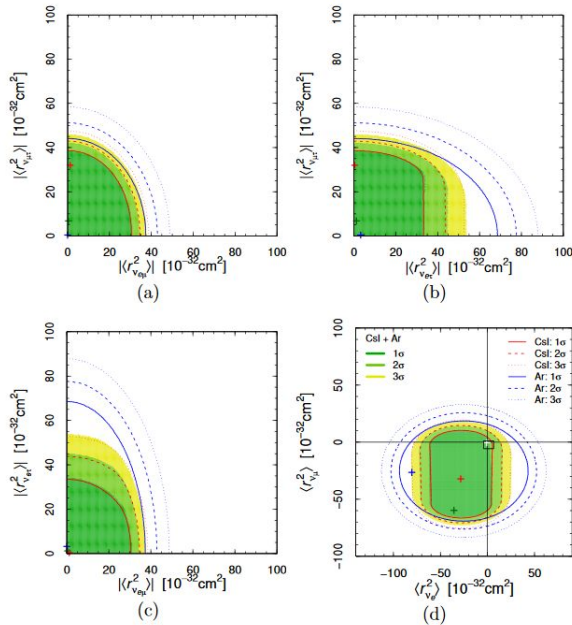


FIG. 5. Contours of the allowed regions in different planes of the neutrino charge radii parameter space obtained with fixed R_n obtained from the analysis of COHERENT Csl data (red lines), from the analysis of COHERENT Ar data in this paper (blue lines), and from the combined fit (shaded green-yellow regions). The crosses with the corresponding colors indicate the best fit points. The white cross near the origin in panel (d) indicates the Standard Model values in Eqs. (10) and (11). The black rectangle near the origin shows the 90% bounds on $\langle r_{\nu_e}^2 \rangle$ and $\langle r_{\nu_\mu}^2 \rangle$ obtained, respectively, in the TEXONO [65] and BNL-E734 [66] experiments.

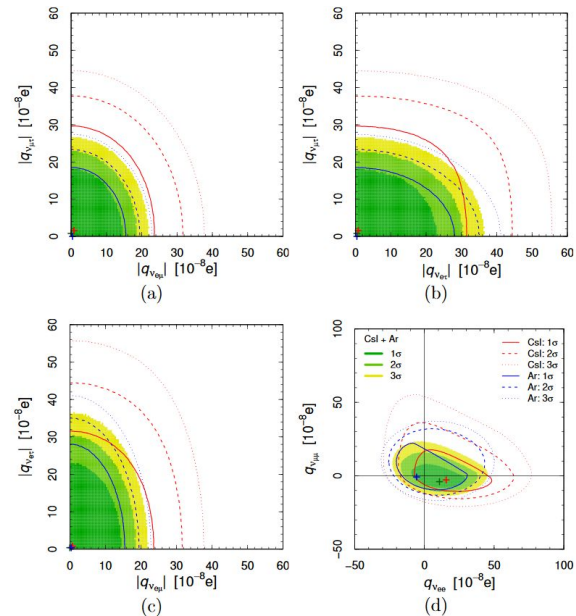


FIG. 8. Contours of the allowed regions in different planes of the neutrino electric charge parameter space obtained with fixed R_n obtained from the analysis of COHERENT Csl data (red lines), from the analysis of COHERENT Ar data in this paper (blue lines), and from the combined fit (shaded green-yellow regions). The crosses with the corresponding colors indicate the best fit points.

Light vector and scalar mediators

Implications of the first detection of coherent elastic
neutrino-nucleus scattering (CEvNS) with Liquid Argon

O. G. Miranda,^{1,*} D. K. Papoulias,^{2,†} G. Sanchez Garcia,^{1,‡}
O. Sanders,^{1,§} M. Tórtola,^{3,¶} and J. W. F. Valle^{3,**}

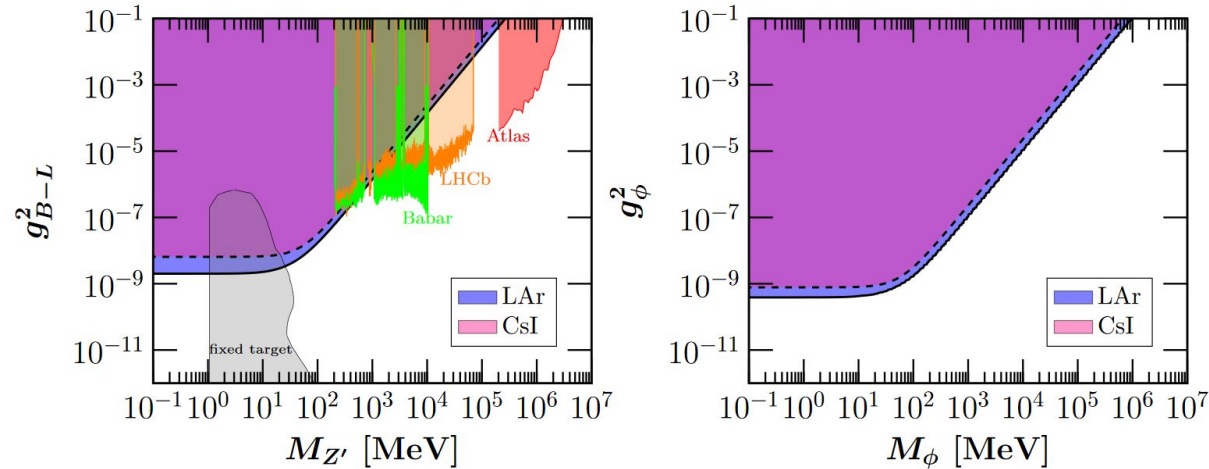
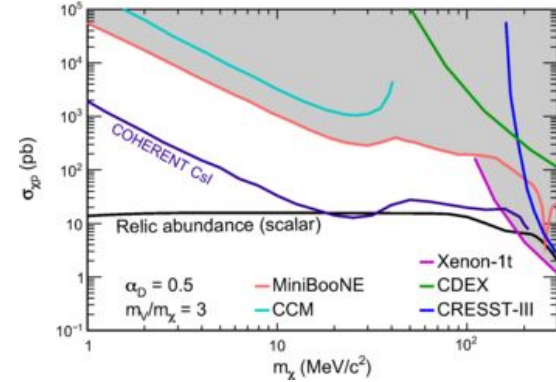
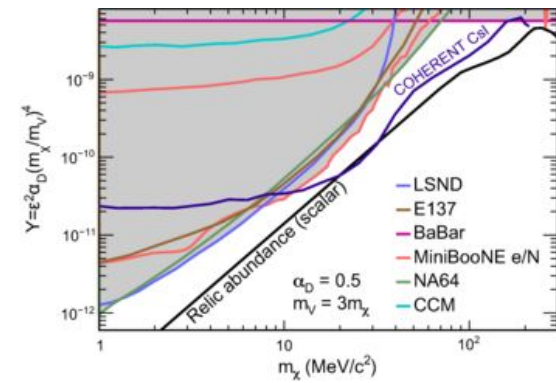
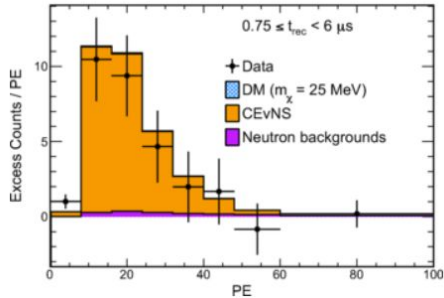
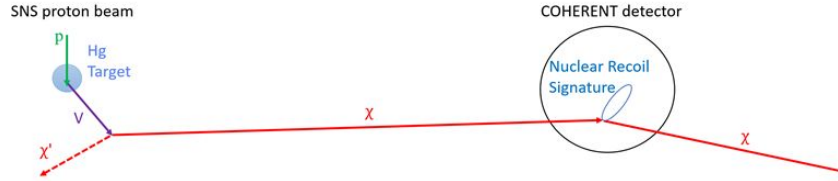
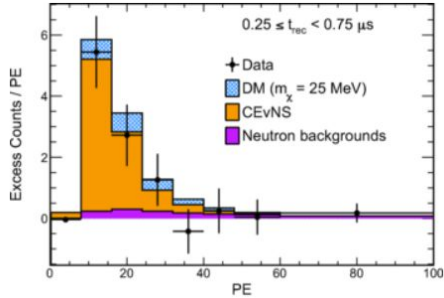


FIG. 7: Excluded region at 90% C.L in the parameter space $(M_{Z'}, g_{B-L}^2)$ for the vector mediator scenario (left) and (M_ϕ, g_ϕ^2) for the scalar mediator scenario (right), from the analysis of the recent LAr data. In both cases, a comparison is given with the CsI data.

Accelerator-produced DM

- Vector-portal dark matter from neutral mesons in target
- Prompt
- Recoil spectrum depends upon mediator mass
- Coherent nuclear enhancement



First Probe of Sub-GeV Dark Matter beyond the Cosmological Expectation with the COHERENT CsI Detector at the SNS

D. Akimov *et al.*
Phys. Rev. Lett. **130**, 051803 – Published 3 February 2023

Sensitivity of the COHERENT experiment to accelerator-produced dark matter

D. Akimov *et al.*
Phys. Rev. D **102**, 052007 – Published 29 September 2020

Outlook

- Neutrino-nucleus cross section measurements (and improved flux assessments) facilitate an array of BSM searches, provide robust assessments of SN neutrino signals, and contribute to the rich interplay between nuclear physics and the physics of weak interactions
- CEvNS is a “clean” channel for a number of BSM searches and for vector-portal dark-matter searches
- Stopped pion sources provide a relatively well characterized source of neutrinos for cross section measurements
- High and ultra-high energy neutrino interaction measurements likewise benefit from both new experiments and refined theoretical evaluations

